Towards the Validation of Novel Tau PET tracer [F-18]-AV-1451 (T807) on Postmortem Brain Tissue

Teresa Gómez-Isla, MD, PhD
Massachusetts General Hospital
Harvard Medical School
Massachusetts ADRC

- Development of novel tau targeting PET tracers opens an exciting opportunity of using them as potential surrogate markers to measure brain tau pathology by *in vivo* imaging.

- Anticipated challenges:

  ✓ Tau deposits are **intracellular**.

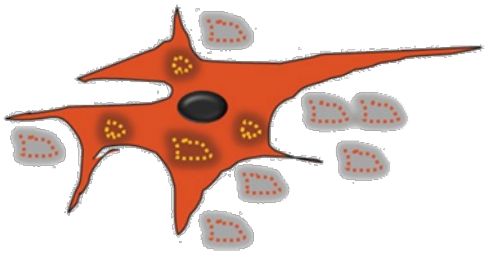

  ✓ Need for tracers with **high binding selectivity** for tau lesions over β-amyloid (Aβ) plaques and other amyloid-like proteins able to form deposits with a β-pleated sheet conformation.

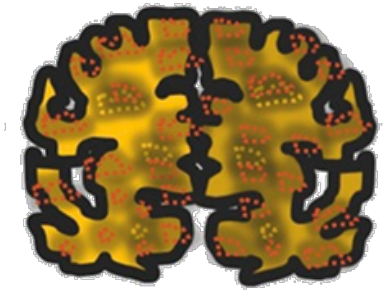

Aß plaques coexist with Tau tangles: [Aß] >> [Tau]

J Nucl Med 2014 Shah & Catafau

•Differences of brain tau deposits in each tauopathy potentially associated with altered ability to be identified by tau PET tracers:

- ✓ **Regional distribution** of tau deposits in the brain

- ✓ **Morphology**:
  - tangles, neuropil threads and dystrophic neurites - AD
  - Pick bodies - PiD
  - Coiled bodies, globose tangles and tufted astrocytes - PSP
  - Astrocytic plaques, coiled bodies and neuropil threads – CBD

- ✓ **Isoform composition**
  - Mixture of 3R+4R - AD
  - 3R - PiD
  - 4R - PSP and CBD

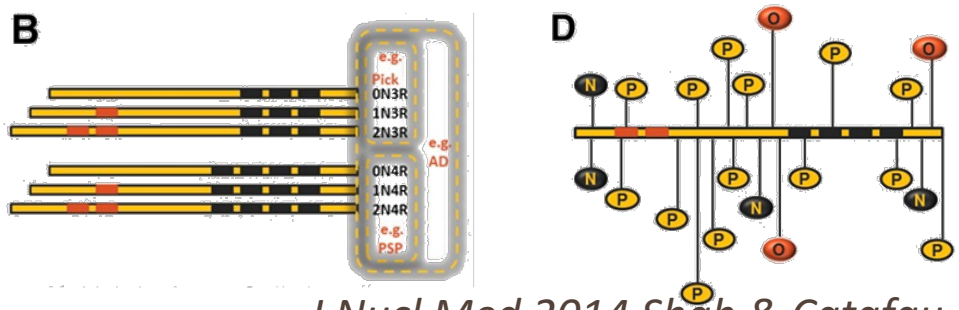

J Nucl Med 2014 Shah & Catafau

- ✓ **Ultrastructural characteristics of tau filaments**
  - Paired helical filaments - AD
  - Straight filaments - PiD, PSP and CBD

Chemical structures of novel tau compounds

Ligand	Structure	Affinity for Tau [nM]	Specificity for Tau relative to Aß	Mouse brain uptake at 2 min [%ID/g]	Mouse brain washout (2min/ 30 min)
^{11}C-PBB3[9]	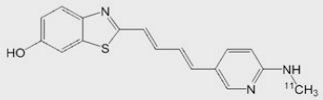	K_{d1}=2.5* K_{d2}=100	40-to-50-fold	NA	NA
^{18}F-THK523[13, 15]	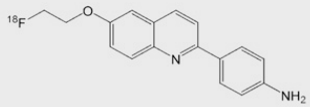	K_{d1}=1.99† K_{d2}=50.7	15-fold	2.72	1.9
^{18}F-THK5105[15]	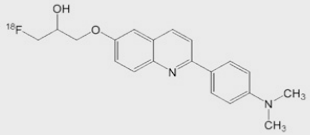	K_{d1}=1.45‡ K_{d2}=7.40	25-fold	9.2	2.6
^{18}F-THK5117[15]	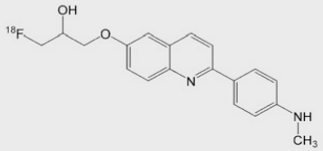	(K_i=10.5)‡	(NA)	6.06	10.3
^{18}F-T807[18]	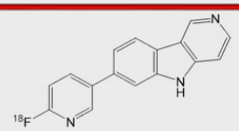	K_d=14.6*	>25-fold	4.16	6.7
^{18}F-T808[17]	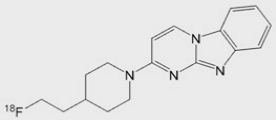	K_d=22*	27-fold	6.7§	2.9ǀ

* K_d determined by ligand-binding to Tau-positive human brain sections
† K_d determined by ligand-binding to Tau-fibrils
‡ K_i determined by competitive inhibition of ^{18}F-THK5105 to Tau-fibrils
§ 2.5 min; ǀ washout 2.5 min/20 min
NA= Not available; N.B. The affinity values for various ligands are generated from different types of experiments and may not always be directly comparable.

J Nucl Med 2014 Shah&Catafau

Journal of Alzheimer's Disease 31 (2012) 601–612
DOI 10.3233/JAD-2012-120712
IOS Press

A Highly Selective and Specific PET Tracer for Imaging of Tau Pathologies

Wei Zhang, Janna Arteaga, Daniel K. Cashion, Gang Chen, Umesh Gangadharmath, Luis F. Gomez, Dhanalakshmi Kasi, Chung Lam, Qianwa Liang, Changhui Liu, Vani P. Mocharla, Fanrong Mu, Anjana Sinha, A. Katrin Szardenings, Eric Wang, Joseph C. Walsh, Chunfang Xia, Chul Yu, Tieming Zhao and Hartmuth C. Kolb*
Siemens Molecular Imaging, Inc., Culver City, CA, USA

- Screening of hundreds of compounds, originally designed to bind Aβ deposits, carbazoles yielded good candidates for selective tau binding – T726 (fluorescent).

- *In vivo* and *in vitro* properties of T726 were optimized further. A close analogue, AV-1451 (T807), designed to specifically bind PHF-tau, emerged as the lead candidate.

- AV-1451 (T807) and T726 structures are not identical.

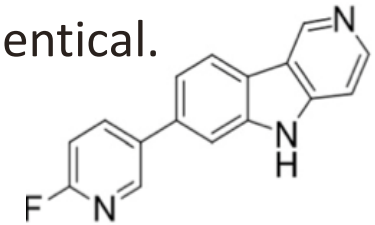

T807

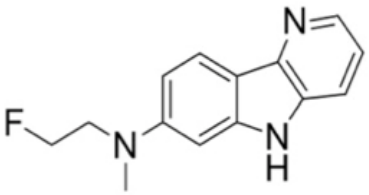

T726

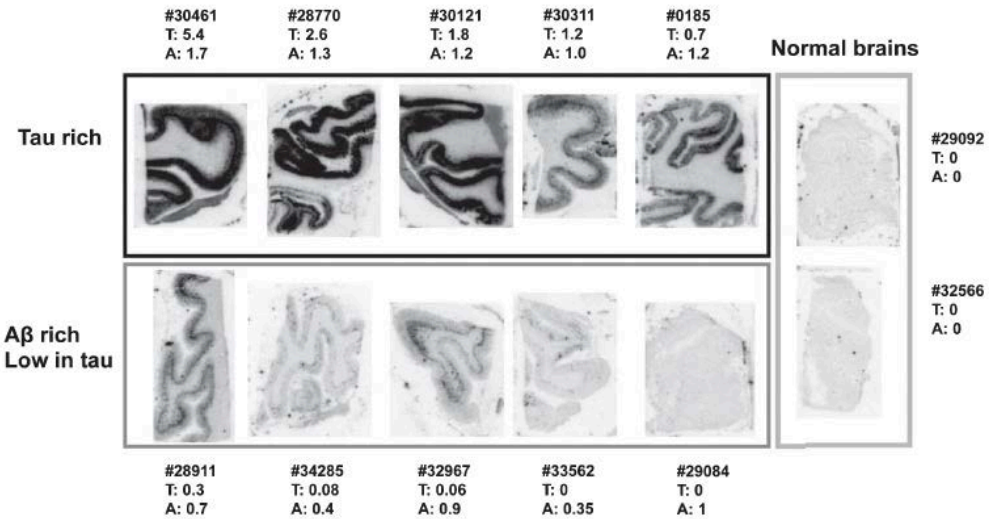

Correlation of [F-18]-AV-1451 ARG and PHF1/Aβ IHC

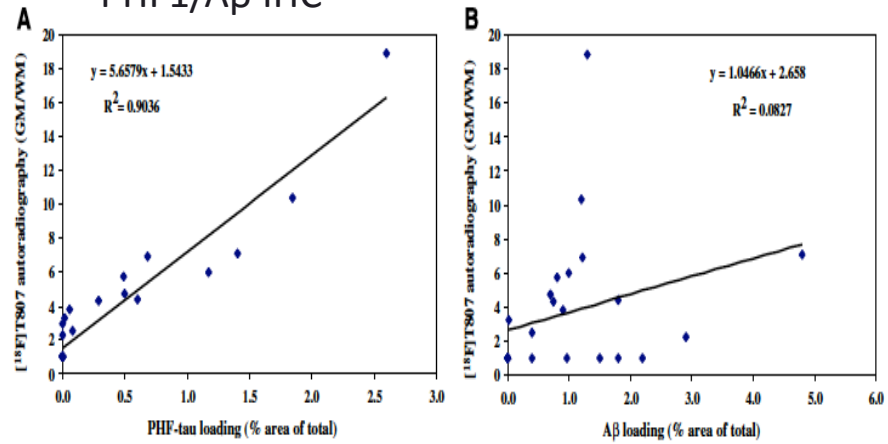

- >25 fold selectivity for PHF-tau over Aβ
- Good overlap with PHF staining but not with Aβ
- Little white matter binding
- Non-detectable/minimal off-target binding

[^{18}F]T807, a novel tau positron emission tomography imaging agent for Alzheimer's disease

Chun-Fang Xia, Janna Arteaga, Gang Chen, Umesh Gangadharmath, Luis F. Gomez, Dhanalakshmi Kasi, Chung Lam, Qianwa Liang, Changhui Liu, Vani P. Mocharla, Fanrong Mu, Anjana Sinha, Helen Su, A. Katrin Szardenings, Joseph C. Walsh, Eric Wang, Chul Yu, Wei Zhang, Tieming Zhao, Hartmuth C. Kolb*

Molecular Imaging Biomarker Research, Siemens Medical Solution USA, Inc, Culver City, CA, USA

Journal of Alzheimer's Disease 34 (2013) 457–468
DOI 10.3233/JAD-122059
IOS Press

Early Clinical PET Imaging Results with the Novel PHF-Tau Radioligand [F-18]-T807

David T. Chien[a], Shadfar Bahri[b], A. Katrin Szardenings[a], Joseph C. Walsh[a], Fanrong Mu[a], Min-Ying Su[b], William R. Shankle[c], Arkadij Elizarov[a] and Hartmuth C. Kolb[a,*]
[a]*Siemens Molecular Imaging, Inc., Culver City, CA, USA*
[b]*Tu and Yuen Center for Functional Onco-Imaging, Department of Radiological Sciences, University of California Irvine, CA, USA*
[c]*Shankle Clinic Memory and Cognitive Disorders Program, Hoag Neurosciences Institute, Newport Beach, CA, USA*

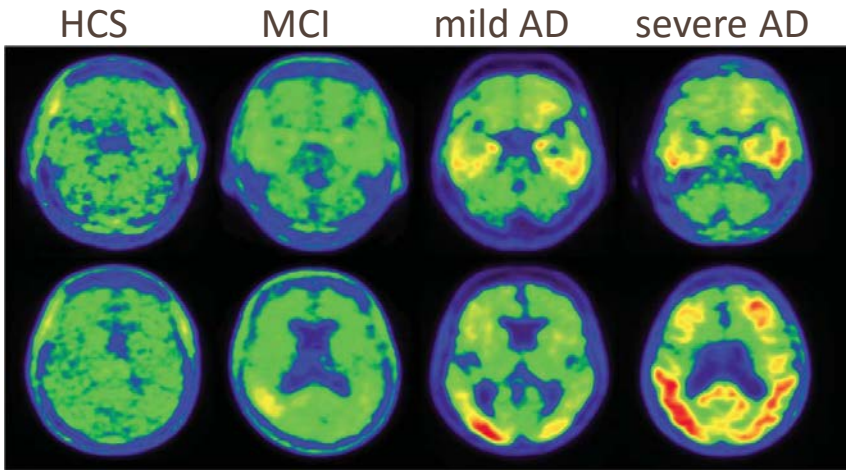

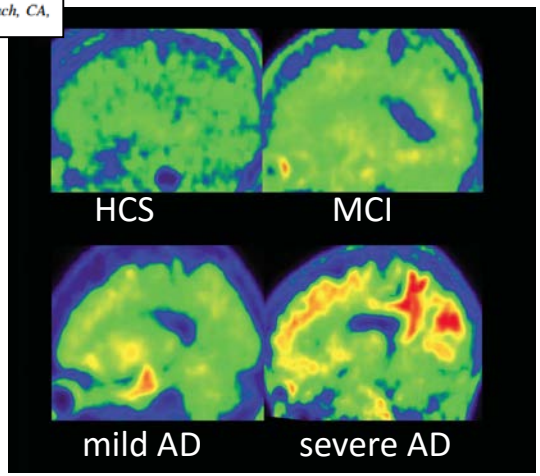

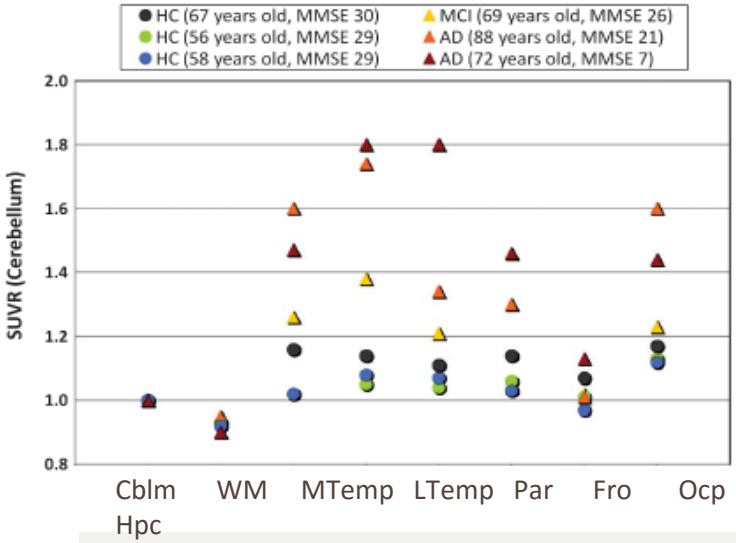

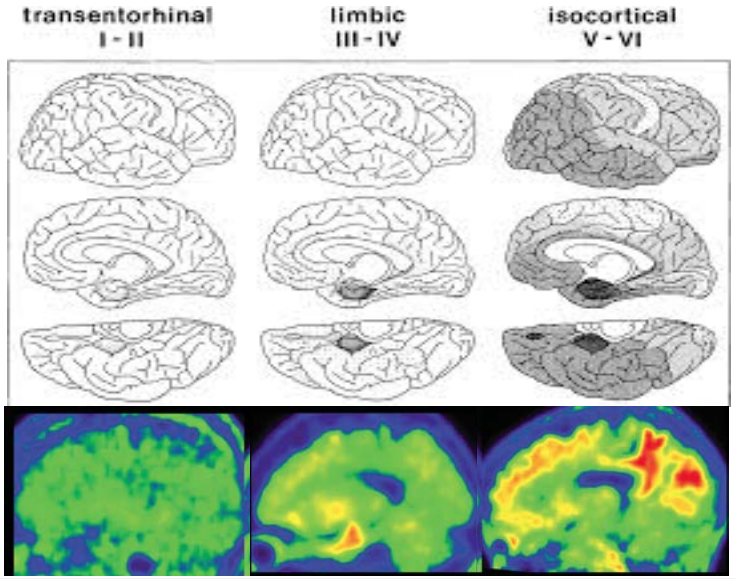

- We aimed at examining region and substrate specific autoradiographic binding patterns of [F-18]-AV-1451 in brain postmortem tissue samples representing a diverse spectrum of neurodegenerative diseases in order to:
    - **Validate the site/s of [F-18]-AV-1451 binding.**
    - **Determine whether there is any off-target binding.**

Early time in tau imaging, yet this compound is quickly making its way into use in clinical research including secondary prevention trials in AD like the A4 trial.

Cases (n=24)

- Alzheimer's disease (n=3)
- Frontotemporal dementia-tau :
  - ✓ Pick disease (n=3)
  - ✓ Progressive supranuclear palsy (n=3)
  - ✓ Corticobasal degeneration (n=2)
- Dementia with Lewy bodies (n=3)
- Multiple System Atrophy (n=1)
- Frontotemporal dementia-TDP-43 (n=1)
- CAA, Iowa D23N APP mutation (n=1)
- Healthy controls (n=2)
- Metastatic melanoma (n=1)
- Superficial siderosis (n=1)
- Hemorrhages (n=3)

Brain regions

- Frontal cortex
- Parietal cortex
- Temporal cortex
- Occipital cortex
- Hippocampus/entorhinal cortex
- Insula
- Cingulate
- Basal ganglia
- Subcortical white matter
- Midbrain
- Pons
- Cerebellar cortex
- Dentate nucleus
- Leptomeninges

(1) [F-18]-AV-1451 phosphor screen autoradiography

- Frozen sections thawed + fixed with Methanol x 20min
- [F-18]-AV-1451 (20µCi/ml) 60min incubation + washes with PBS and EtOH + air dried
- Adjacent sections with identical conditions + unlabeled AV-1451 (1µM) ("blocking") to saturate available tau binding sites
- Phosphor screen (MultiSensitive Phosphor Screen, PerkinElmer Life and Analytic Sciences) overnight
- Imaging system (Cyclone Plus Storage Phosphor Scanner, Perkin Elmer Life and Analytic Sciences)

(2) [F-18]-AV-1451 nuclear emulsion autoradiography

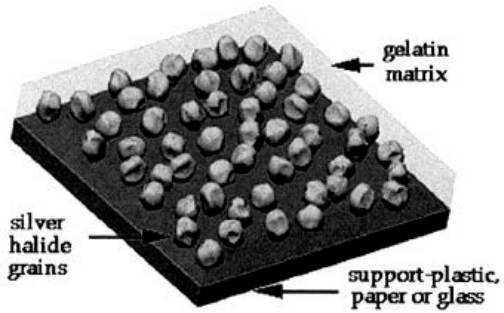

A **photographic nuclear emulsion** consists of a thin layer of radiation-sensitive **silver crystals** suspended in a gelatin matrix which is supported by a glass plate.

When silver grains are struck by radiation (photons or electrons), they are altered chemically to form a latent image of the silver crystals.

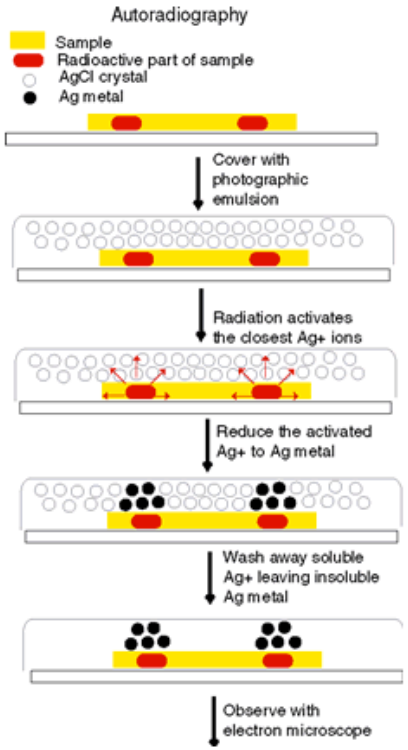

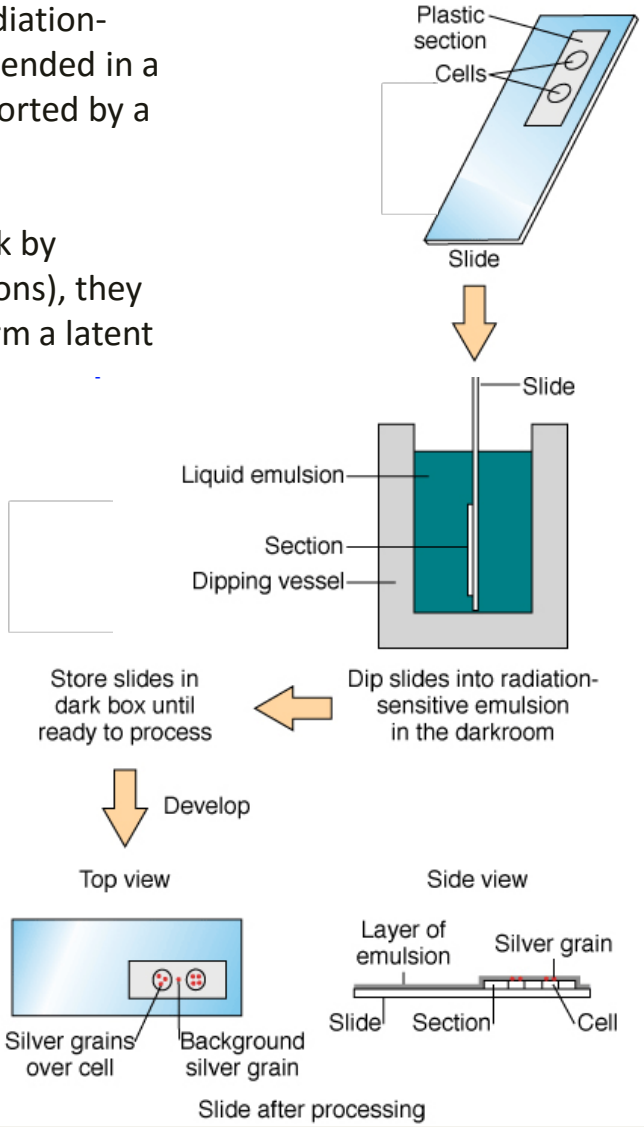

(2) [F-18]-AV-1451 nuclear emulsion autoradiography

- Frozen sections thawed + fixed with Methanol x 20 mins
- [F-18]-AV-1451 (20µCi/ml) 60min incubation + washes with PBS and EtOH + air dried
- Dip the slides x 8 into Ilford photographic emulsion (1:5 in H_2O) in a dark room, left overnight laying flat in a dark box
- The following day: developed with Ilford Phenisol X-ray developer, fixed with Ilford fixative
- Followed by:
  - IHC
  - H&E staining

(3) [H3]-AV-1451 binding assay

•Fresh-frozen human brain samples are homogenized at RT in PBS (137 mM NaCl, 3 mM KCl, 10 mM sodium phosphate, pH 7.0) at a concentration of 10 mg of brain per milliliter.

•10 mg/ml frozen brain homogenate aliquots were thawed and diluted 10-fold in binding buffer to 1 mg/ml.

•500 µl of appropriate concentrations of non-radioactive compound combined with 400 µl of [H-3]-AV-1451 in a volume of 900 ml of binding buffer. The final concentration of [H-3]-AV-1451 is typically 1-2 nM.

•After incubation at RT for 60 min, the binding mixture is filtered through a Whatman GF/B glass filter and washed 5 times with 3 ml binding buffer.

•Filters are counted in Cytoscint-ES after sitting in the cocktail overnight.

•Complete (100%) inhibition of binding is defined as the number of counts displaced by 3 µM non-radioactive T807.

(1) [F-18]-AV-1451 phosphor screen autoradiography: AD vs controls

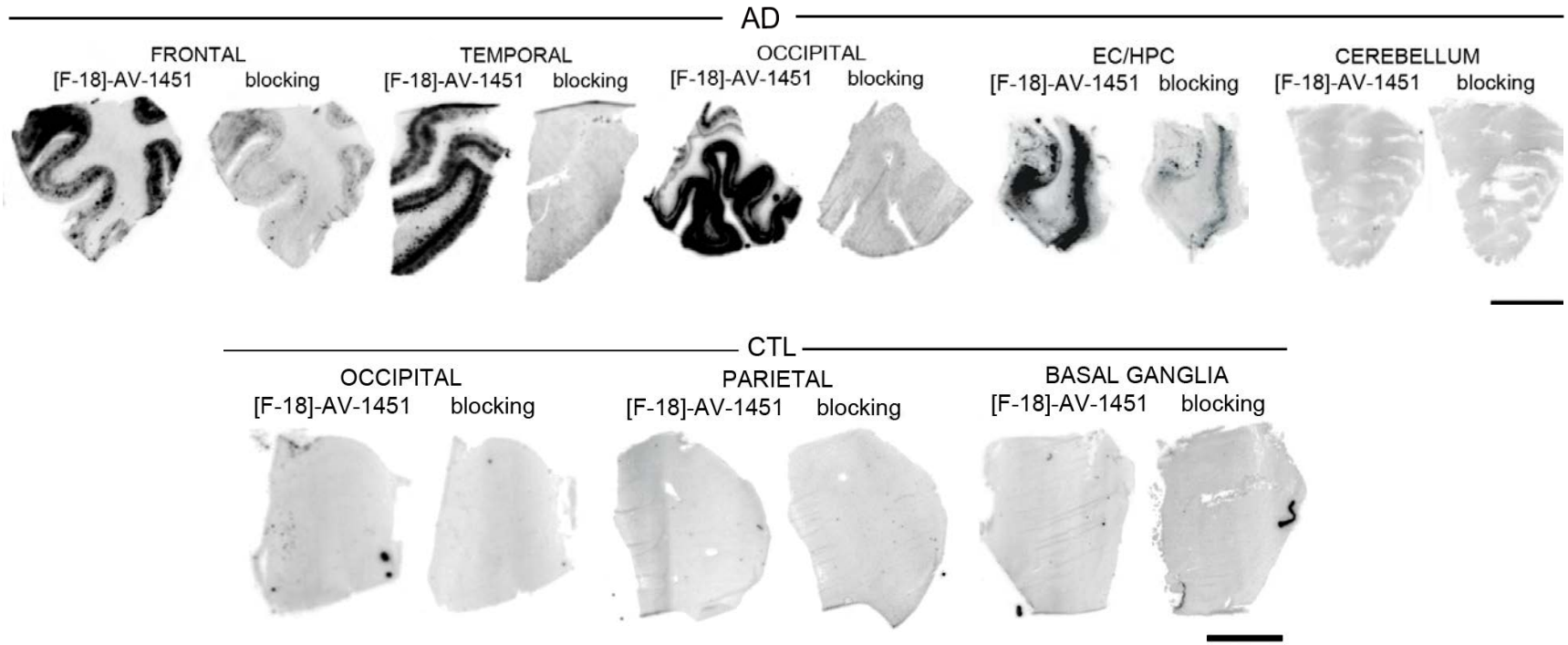

Marquie et al. Ann Neurol 2015

Very strong binding in the HF and EC, frontal , temporal, parietal and occipital cortices in brain slices containing robust loads of NTF from AD brains. Binding was almost completely blocked by cold tracer. No binding in control brains free of NFT pathology.

Tau
(AV-1451)

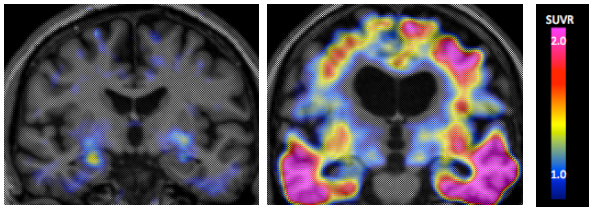

Normal AD dementia

PET images are courtesy of Dr. Keith Johnson

(1) [F-18]-AV-1451 phosphor screen autoradiography: non-AD tauopathy cases

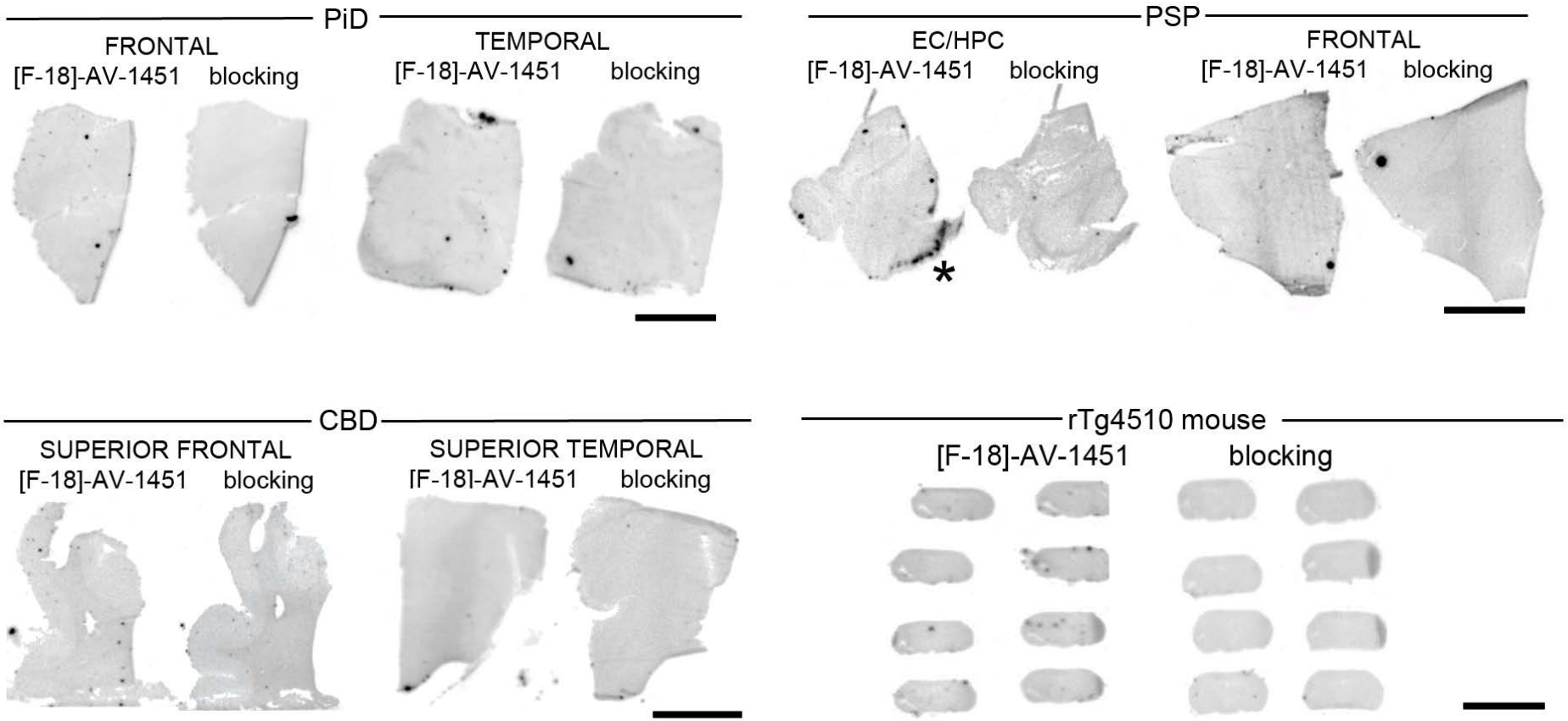

Marquie et al. Ann Neurol 2015

Absence of detectable AV-1451 binding in slices containing non-PHF-tau lesions, except for incidental binding to age-related NFT in the EC (Braak stage II).

No labeling in brains of aged rTg4510 mice containing innumerable P301L (4R) tau lesions.

(1) [F-18]-AV-1451 phosphor screen autoradiography: non-tauopathy cases

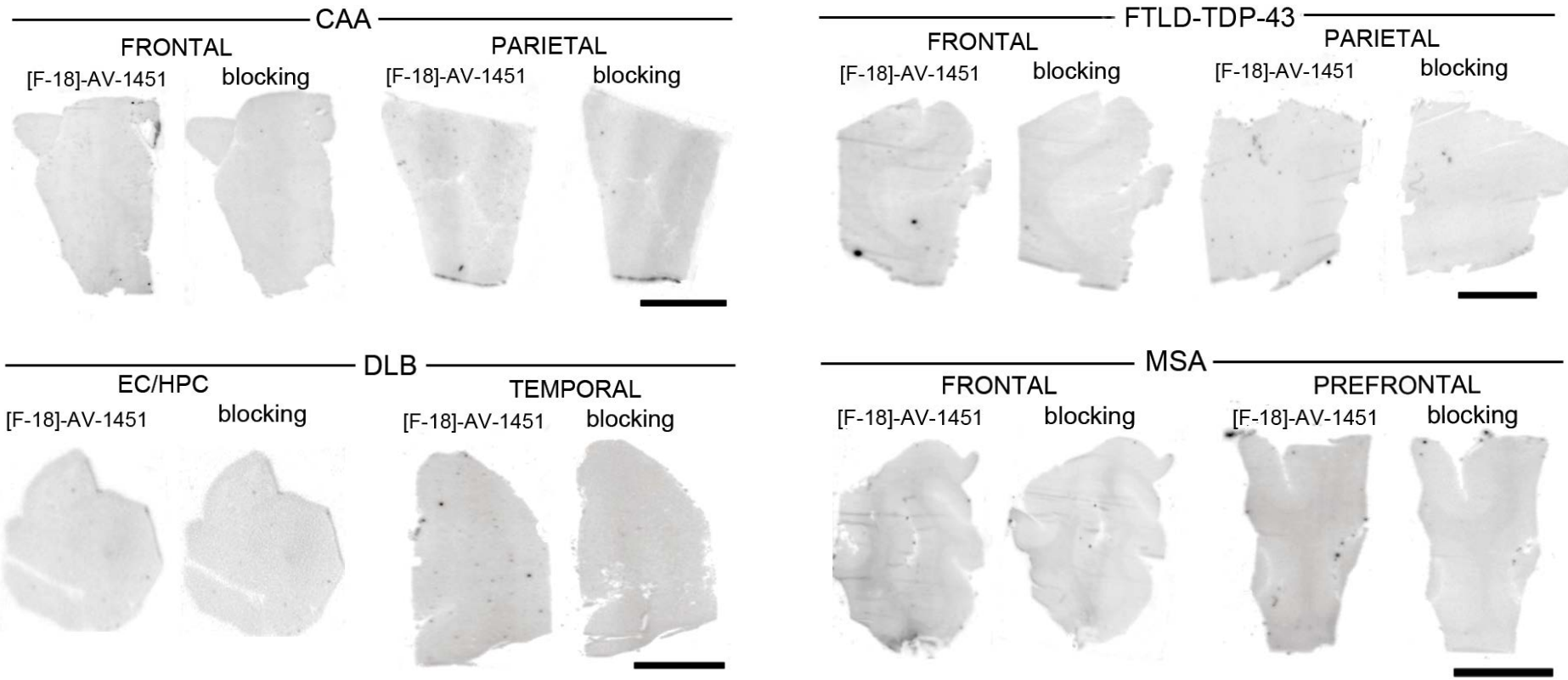

Marquie et al. Ann Neurol 2015

No detectable AV-1451 autoradiographic signal in slices from CAA (D23N Iowa APP mutation), DLB, MSA and FTLD-TDP-43 cases.

(2) [F-18]-AV-1451 nuclear emulsion autoradiography

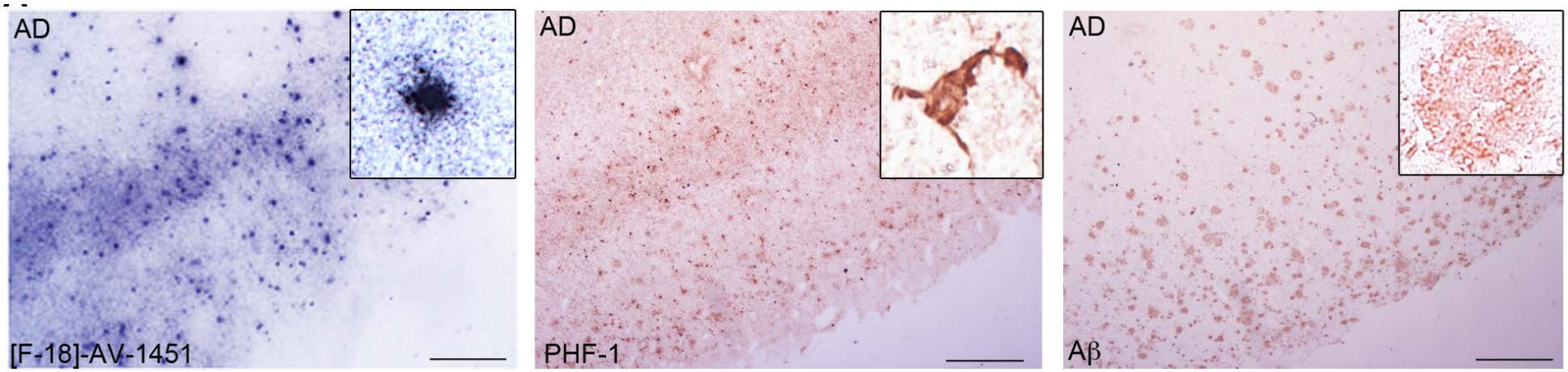

Marquie et al. Ann Neurol 2015

Dipping of adjacent brain slices in photographic nuclear emulsion showed strong and selective concentration of silver grains in gray matter of AD brains, reflecting underlying [F-18]-AV-1451 binding.

Laminar distribution of silver grains closely mirrored PHF-1 immunostaining.

(2) [F-18]-AV-1451 nuclear emulsion autoradiography: PHF-tau deposits

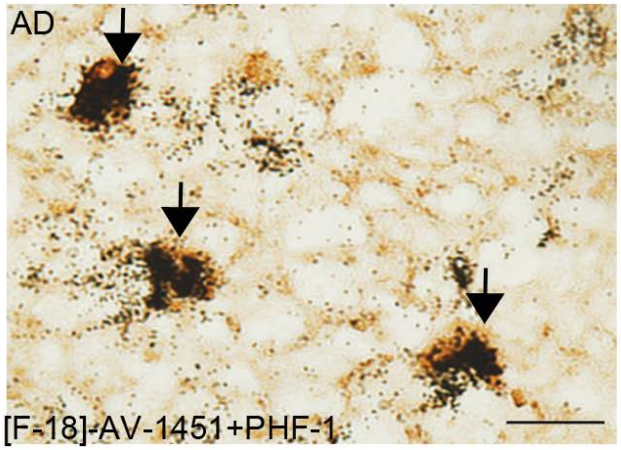

NFT

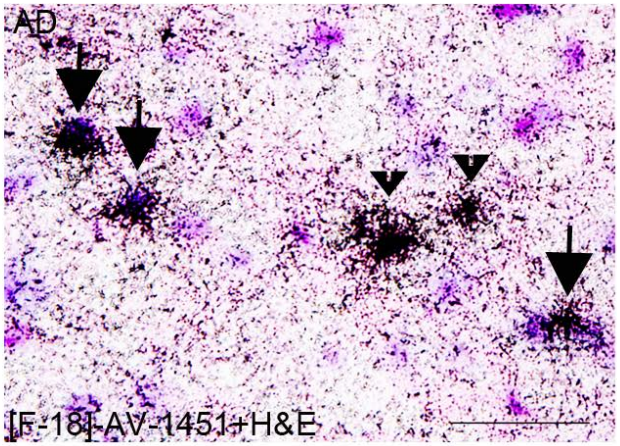

NFT

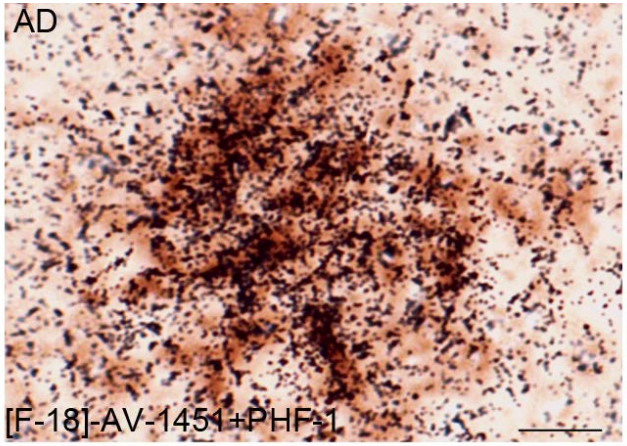

PHF-tau containing dystrophic neurites

Nuclear emulsion followed by IHC further confirmed that [F-18]-AV-1451-labeled lesions were PHF-tau containing deposits, including classic NFT (intra and extraneuronal) and PHF-tau containing neurites.

These lesions likely account for the majority of the observed in vivo signal in patients with AD.

Marquie et al. Ann Neurol 2015

AD DEMENTIA

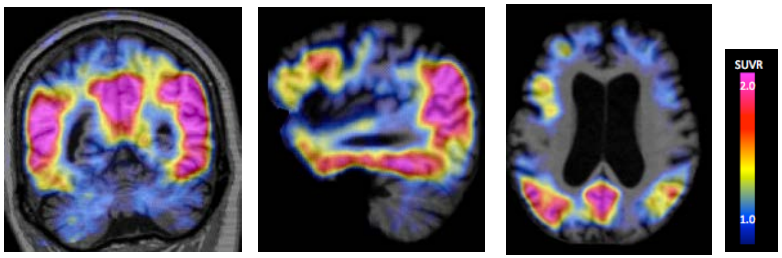

PET images are courtesy of Dr. Keith Johnson

(2) [F-18]-AV-1451 nuclear emulsion autoradiography: Aβ deposits

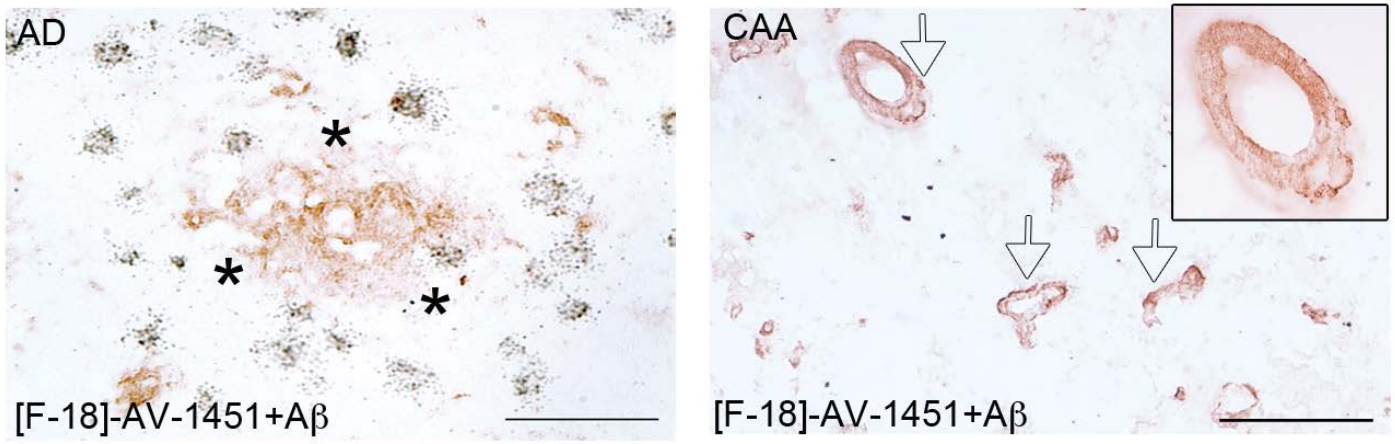

Aβ plaques

CAA

No silver grains colocalizing with Aβ deposits in the form of plaques or CAA.

Marquie et al. Ann Neurol 2015

(2) [F-18]-AV-1451 nuclear emulsion autoradiography: other tau deposits and α-synuclein and TDP-43 inclusions

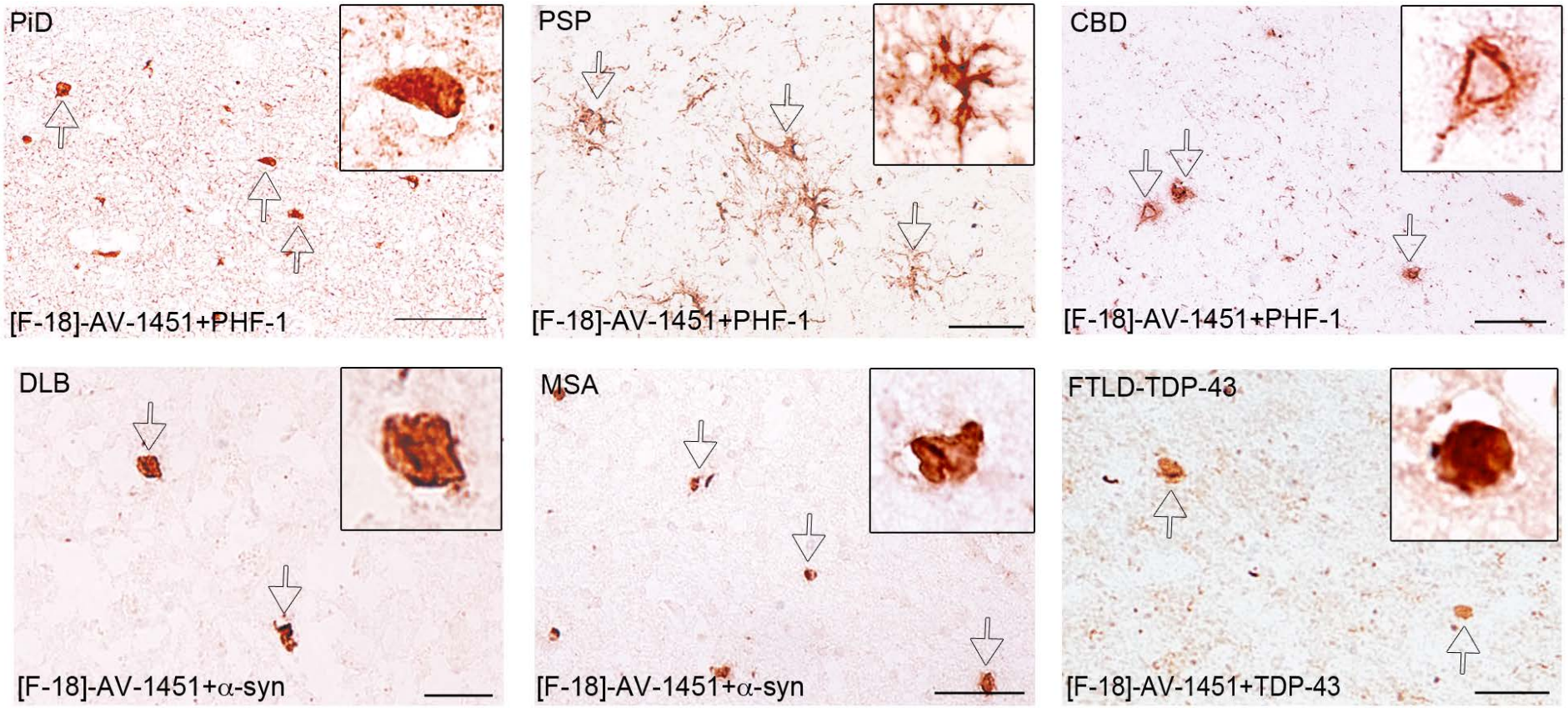

Negligible number of silver grains/no grains colocalizing with tau deposits in PiD, PSP and CBD cases, or with inclusions containing α-synuclein or TDP-43.

Marquie et al. Ann Neurol 2015

Intriguing but frequent findings emerging from early [F-18]-AV-1451 PET imaging studies

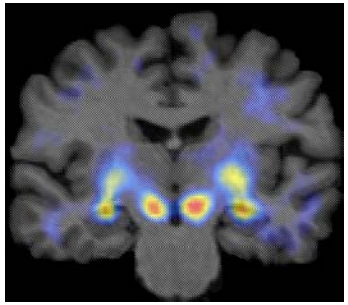

Normal

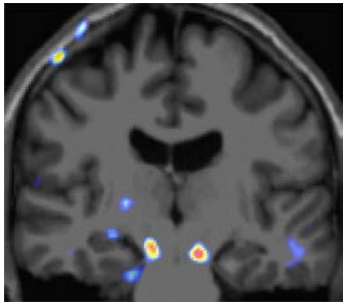

Normal

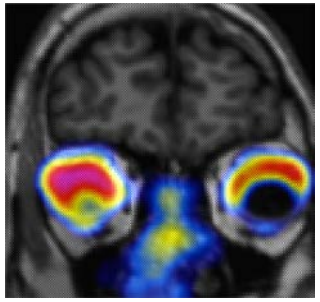

Normal

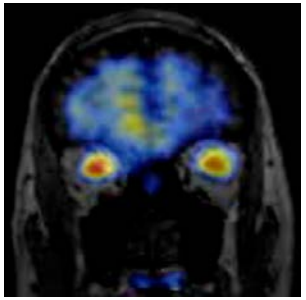

Normal

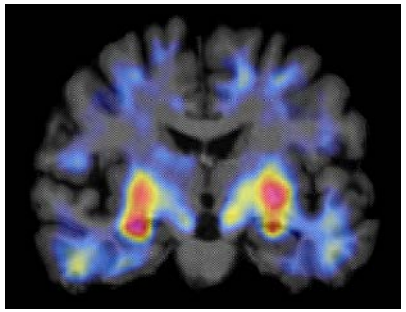

Normal

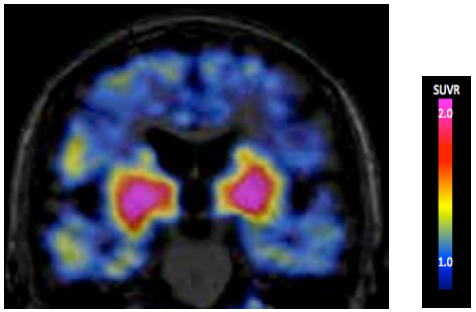

PSP

PET images are courtesy of Dr. Keith Johnson

(1) [F-18]-AV-1451 phosphor screen autoradiography: off-target binding in the midbrain

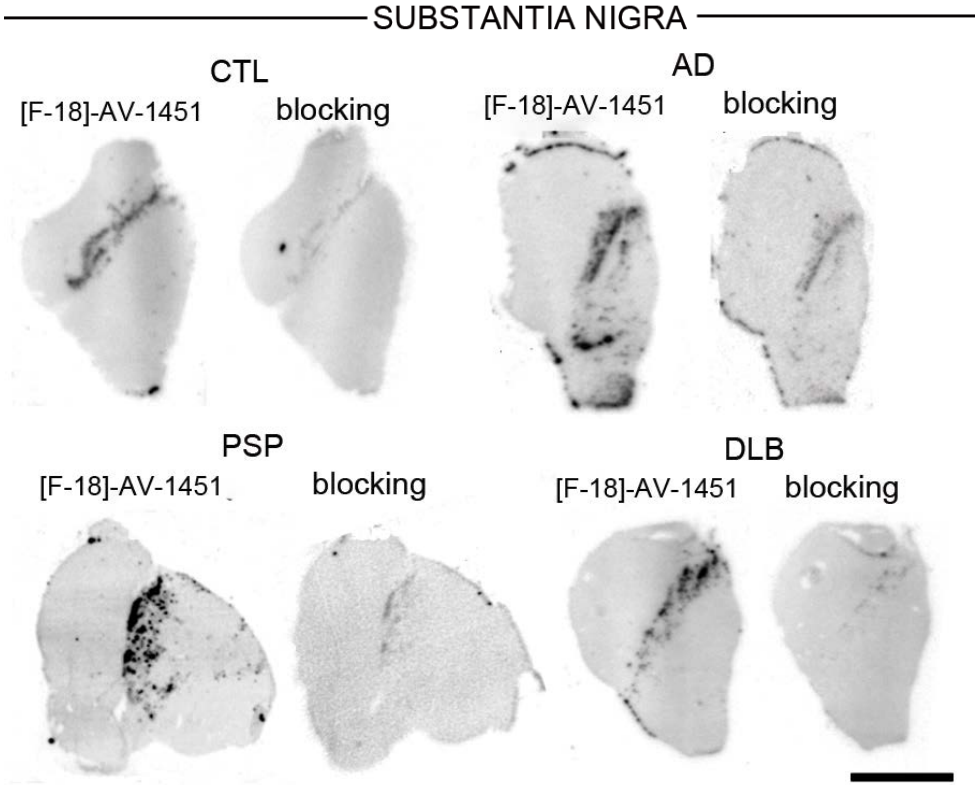

Marquie et al. Ann Neurol 2015

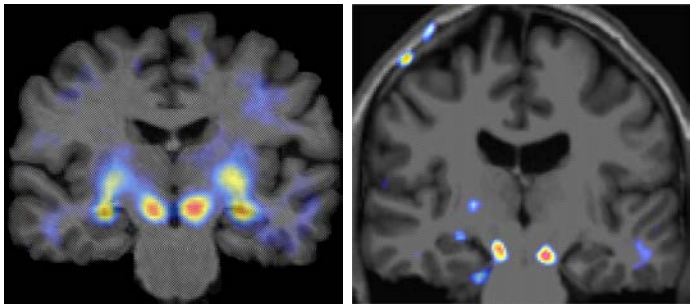

Normal Normal

PET images are courtesy of Dr. Keith Johnson

Strong binding of [F-18]-AV-1451 to midbrain slices containing substantia nigra regardless of the presence of underlying tau deposits.

Binding is almost completely blocked after incubation with unlabeled AV-1451.

(2) [F-18]-AV-1451 autoradiography: off-target binding to neuromelanin- and melanin-containing cells

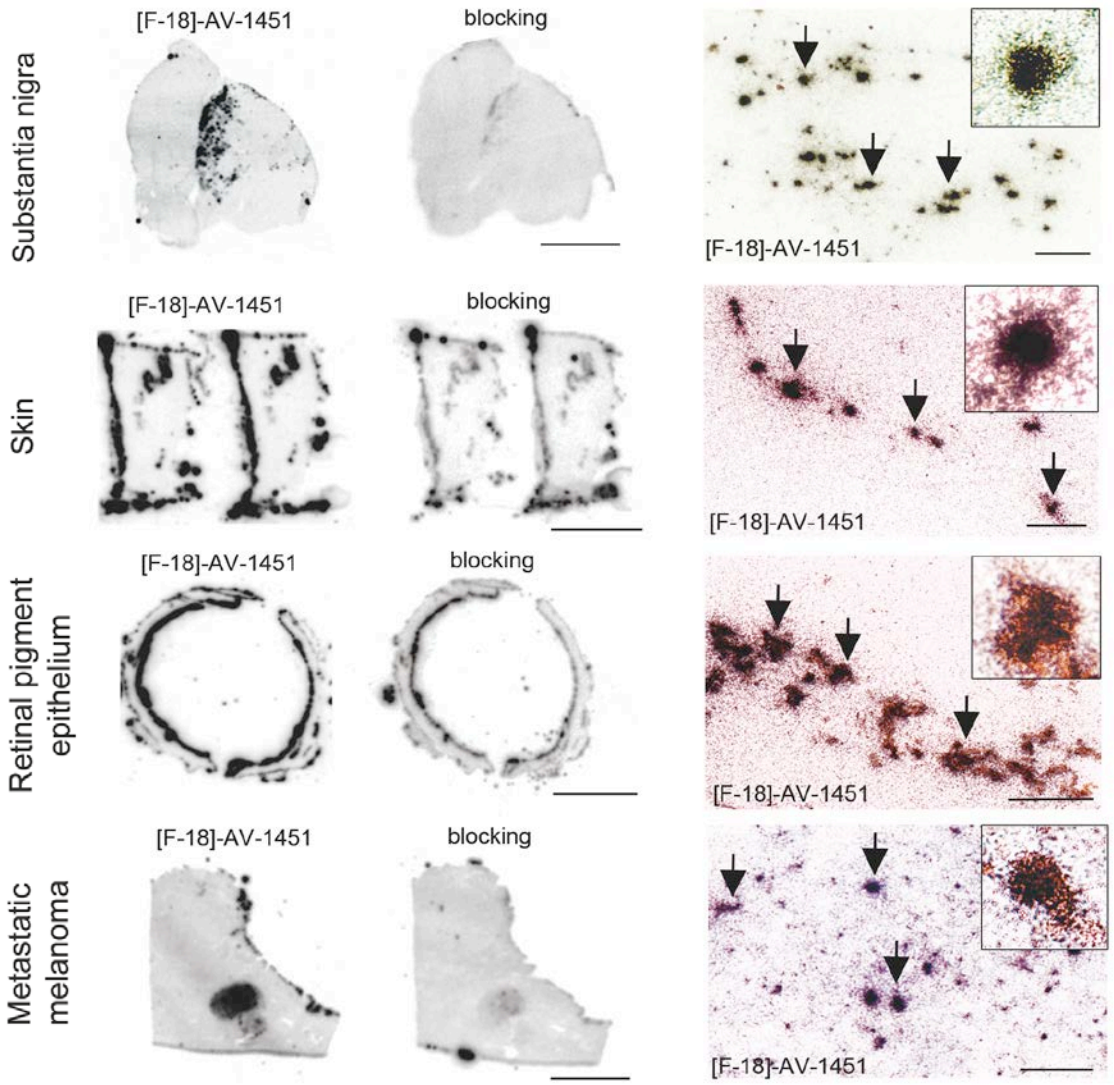

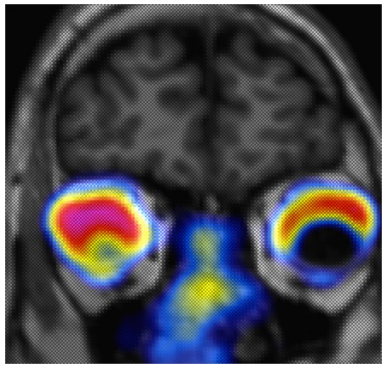

Marquie et al. Ann Neurol 2015

(2) [F-18]-AV-1451 autoradiography: weaker off-target binding to brain hemorrhagic lesions

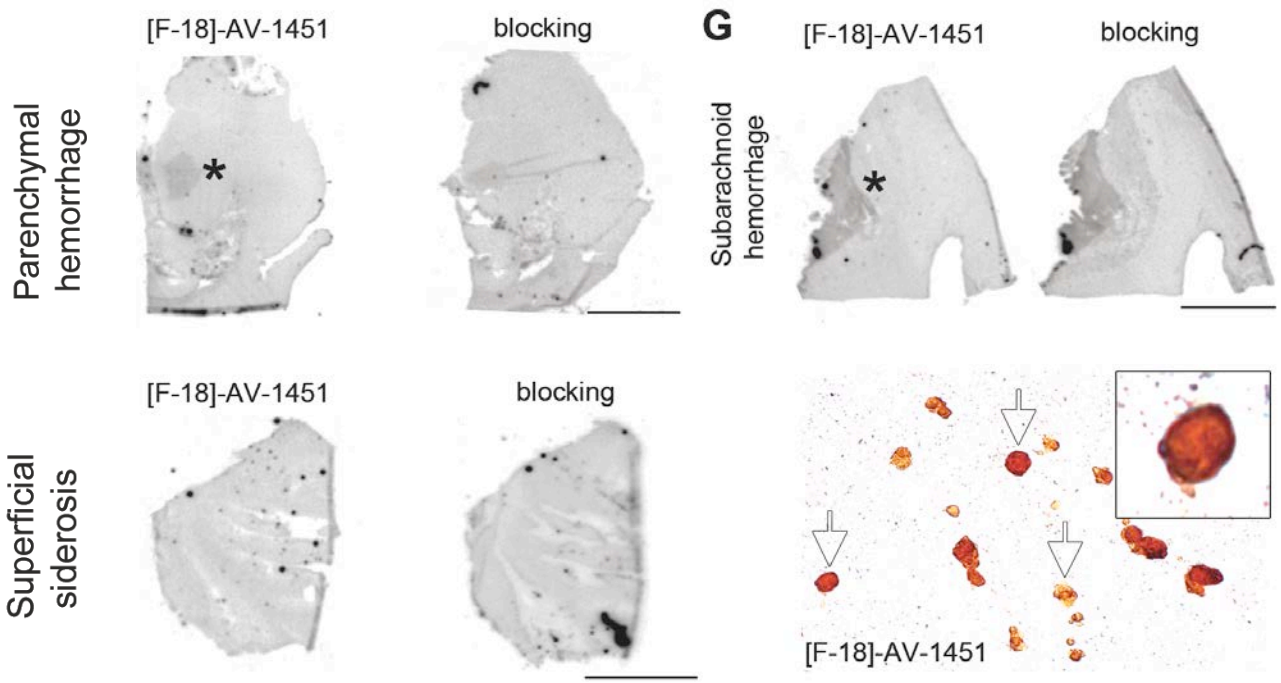

Some [F-18]-AV-1451 binding in brain slices containing recent brain hemorrhagic lesions but no detectable binding to iron deposits.

Marquie et al. Ann Neurol 2015

(1) [F-18]-AV-1451 phosphor screen autoradiography: basal ganglia

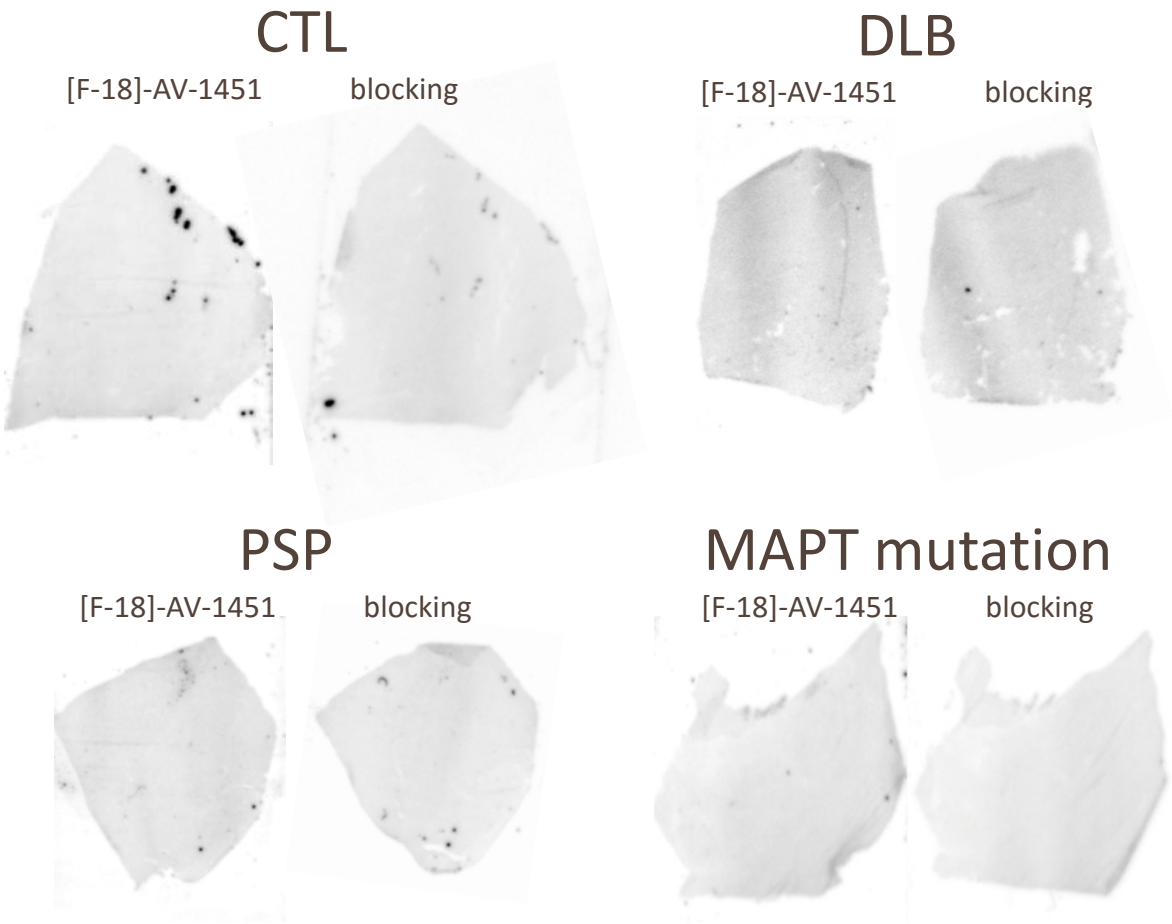

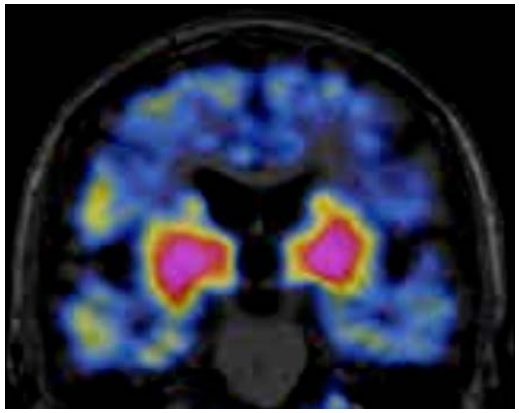

In vivo tracer uptake in basal ganglia may represent nonspecific binding influenced by biological or technical factors other than underlying tau pathology.

(2) [H-3]-AV-1451 binding assay:

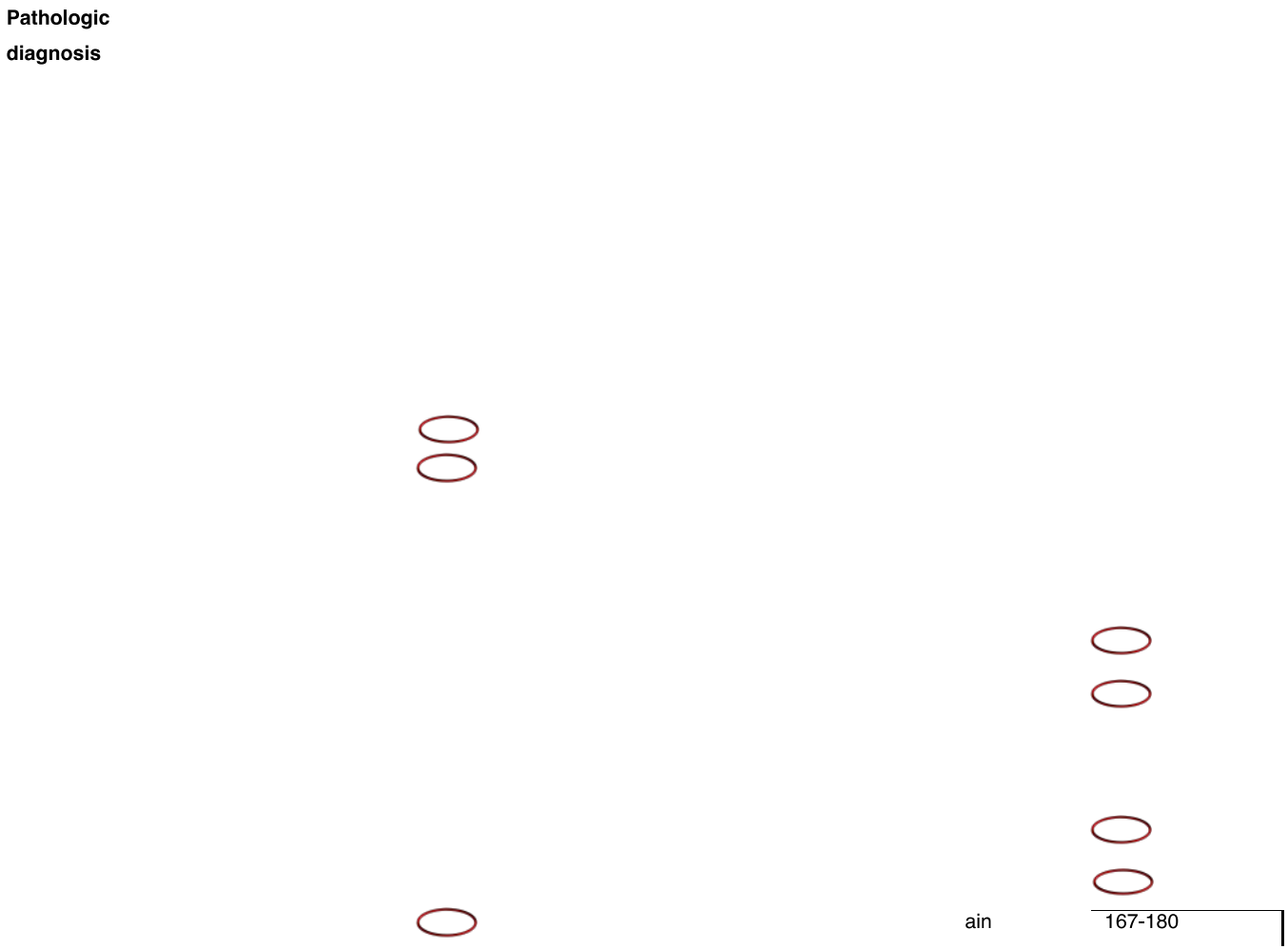

Marquie et al. Ann Neurol 2015

Conclusions

- Our data derived from [F-18]-AV-1451-sensitive autoradiography and [H-3]-AV-1451 *in vitro* binding assays suggest that this tracer strongly binds to lesions primarily made of tau in the form of PHF (e g. neurofibrillary tangles and PHF-tau containing neurites).

- [F-18]-AV-1451 does not bind to a significant extent to neuronal and glial inclusions mainly composed of straight tau filaments (non-AD tauopathies) or to Aβ deposits, α-synuclein and TDP-43 inclusions.

- [F-18]-AV-1451 shows strong off-target binding to neuromelanin- and melanin-containing cells, and some weaker off-target binding to brain hemorrhagic lesions.

Acknowledgements

MADRC

Marta Marquie-Sayagues
Charles Vanderburg
Elizabeth Bien
Lisa Rycyna
Matthew Frosch
Bradley Hyman
Keith Johnson
Bradford Dickerson
Stephen Gomperts
Isabel Costantino
Chris William

Radiology Department-MGH

Marc Normandin

ADRC University of Pittsburgh

Bill Klunk
Chester Mathis
Milos Ikonomovic
Manik Debnath

Funding support :

- NIH Grant U01 AG016976
- NIH Grant R01 AG43511
- P50AG016574
- ASISA foundation, Spain

*Avid/Lilly provided AV-1451 fluorescent analogues
* Dr. Peter Davies kindly provided PHF1 antibody

How do we reconcile our findings with some findings communicated by others from early [F-18]-AV-1451 PET imaging studies in PSP patients?